

THE EVOLUTION OF PROTOPLANETARY DISKS WITH VARIED INITIAL CONDITIONS. S. Michael, A. C. Boley, R. H. Durisen, *Department of Astronomy, Indiana University, Bloomington IN 47405-7105, USA, (scamicha@indiana.edu).*

Introduction: The effects of gravitational instabilities (GIs) on protoplanetary disk evolution and planet formation have been studied by many authors [e.g., 1-7]. Due to the highly nonlinear nature of the problem, the studies, for the most part, have relied heavily on numerical simulations. As a result, most simulations assume some initial distribution of surface density and temperature. We present a series of three-dimensional hydrodynamics simulations of protoplanetary disks with varied initial surface densities to study how initial conditions influence GIs and protoplanetary disk evolution.

Numerics: The code is second-order in space and time and solves the equations of hydrodynamics on a Eulerian cylindrical grid [5]. Three different initial surface density profiles $\Sigma \propto r^{-1/2}$ (shallow), $\Sigma \propto r^{-1}$ (moderate), and $\Sigma \propto r^{-3/2}$ (steep), are generated using a grid-based self-consistent field scheme [6]. The initial equilibrium models have a central star with mass $0.5M_{\odot}$ and a disk mass of $0.07M_{\odot}$. They also have the equation of state of an isentropic monatomic ideal gas. The isentropic condition combined with the chosen surface density profiles give initial midplane temperature profiles $T \propto r^{-1}$, $T \propto r^{-5/4}$, and $T \propto r^{-3/2}$ for the shallow, moderate, and steep calculations, respectively. In each of the models, the Toomre $Q = c_s \kappa / \pi G \Sigma$ [8] has a minimum value of about 2. In order to model the effects of cooling, we use a global constant cooling time set to approximately 500 years. Artificial bulk viscosity is used to simulate shock heating. The initial disks extend from 2 to 40 AU, and have a grid resolution of $(r, \phi, z) = (256, 128, 32)$ above the midplane.

Results: Each simulation proceeds through similar phases, regardless of the surface density profile. The disk begins in axisymmetry and cools until it becomes unstable; it then undergoes a burst of GI activity, which generates nonaxisymmetric structure and heating due to spiral shocks. This *burst phase* transitions to an *asymptotic phase* of sustained GIs where heating by shocks is roughly balanced by cooling. During the latter phase, the majority of the disk has a Q -value that hovers near instability, i.e. $Q \approx 1.5$ [2], regardless of the initial surface density profile. As in Mejía et al. [7], the GI-induced structure in our disks is dominated by low-order global modes.

Figures 1-3 are midplane density maps for the end of each simulation; all three have well-developed rings in the inner disk. The outermost ring at about 10 to 12 AU is due to a transition from a GI-inactive inner region to a GI-inactive outer region where gravitational torques generated by the GIs act to transport mass inward. Where the disk becomes GI-inactive, this transport is halted, causing the mass to pile up and form a ring. The boundary ring in the shallow simulation is much weaker than the rings in the other two cases because less mass is available in the inner disk. Various other rings can be seen to have formed inside this boundary ring. These may be caused by resonances with spiral modes in the outer disk [9] or, perhaps, by edge modes [see 10]. In all the simulations,

by the time the asymptotic state is reached, the GIs redistribute the mass so that the surface density in the outer disk is quite steep, $\Sigma \propto r^{-5/2}$.

Despite these overall similarities, there are some differences in the evolution of each of the simulations. The burst phase occurs earlier and is more violent for the shallow disk than in the other two disks. This is an expected because more of the mass is concentrated in the outer GI-active region. The differences in the burst between the moderate and the steep disks are much less pronounced.

Discussion: A critical ongoing debate [11] in protoplanetary disk theory is whether GIs in real disks behave locally [2, 3] or globally [6, 7]. If the GIs behave locally, then it may be possible to model their effects on mass and angular momentum transport by using a local “ α -disk” prescription [10]. Gammie [2] found that, in a razor-thin disk, an effective α could be calculated based on the cooling time and the ratio of specific heats, $\alpha = [\gamma(\gamma - 1) \frac{9}{4} \Omega t_c]^{-1}$, where Ω is the rotation frequency and t_c is the cooling time. If GIs behave locally, mass transport due to GIs should closely follow this relation. Using a method similar to Lodato & Rice [3] to calculate the gravitational stress tensor [13] and Reynolds stress, we find that the effective α [3] is given by

$$\alpha(r) = \left| \frac{d \ln \Omega}{d \ln r} \right|^{-1} \frac{T_{r\phi}^{\text{grav}} + T_{r\phi}^{\text{Reyn}}}{\Sigma c_s^2}.$$

Figure 4 shows that this effective α calculated for the steep disk is much larger than that given by Gammie’s formula, a result that is at odds with Lodato & Rice [3] but agrees with Mejía et al. [7].

Conclusions: Varying the initial surface density profile affects the strength and onset time of GI activity, but it does not alter the qualitative behavior. All disks exhibit a strong initial burst and transition into an asymptotic phase of sustained GI activity. Mass transport produces rings in the inner disk and similar surface density profiles $\Sigma \propto r^{-5/2}$ in the outer disk. GIs behave globally. Low-order modes dominate, and effective α ’s are much larger than predicted by a local approximation.

References [1] Boss, A.P., 2005, ApJ, submitted [2] Gammie, C. F. 2001, ApJ, 553, 174 [3] Lodato, G., & Rice, W. K. M. 2004, MNRAS, 351, 630 [4] Mayer, L., Quinn, T., Wadsley, J., Stadel, J. 2002, Sci, 298, 1756 [5] Mejía, A. C. 2004, Ph.D. dissertation, Indiana University [6] Pickett, B. K., Mejía, A.C., Durisen, R. H., Cassen, P. M., Berry, D. K., Link, R. P. 2003, ApJ, 590, 1060 [7] Mejía, A. C., Durisen, R. H., Pickett, M. K., Cai, K. 2005, ApJ, 619, 1098 [8] Toomre, A. 1964, ApJ, 139, 1217 [9] Durisen, R. H., Cai, K., Mejía, A. C., Pickett, M. K. 2005, Icarus, 173, 417 [10] Papaloizou, J. C., Savonije, G. J. 1991, MNRAS, 248, 353 [11] Balbus, S. A., Papaloizou, J. C. 1999, ApJ, 521, 650 [12] Shakura, N. I., Sunyaev, R. A. 1973, A&A, 24, 337 [13] Lynden-Bell, D., Kalnajs A. J. 1972, MNRAS, 157, 1

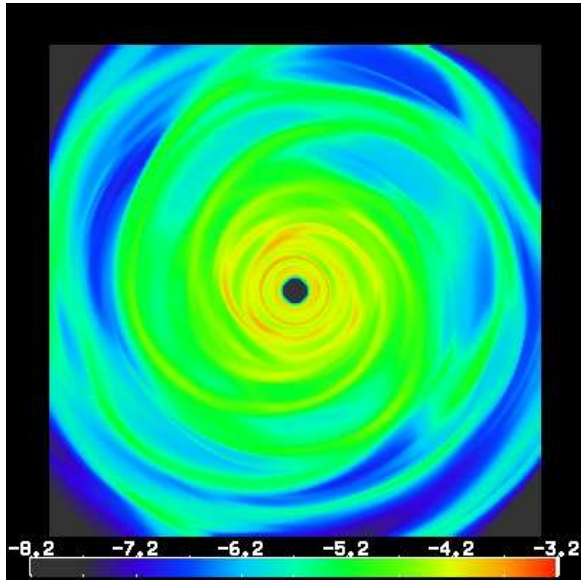


Figure 1: Equatorial density plot for shallow simulation. Scale is logarithmic in arbitrary units. Multiplying by 6.0×10^{-7} gives g/cc. Snapshot is taken at the end of the simulation, in this case about 6000 years. The panel is approximately 100 AU on a side.

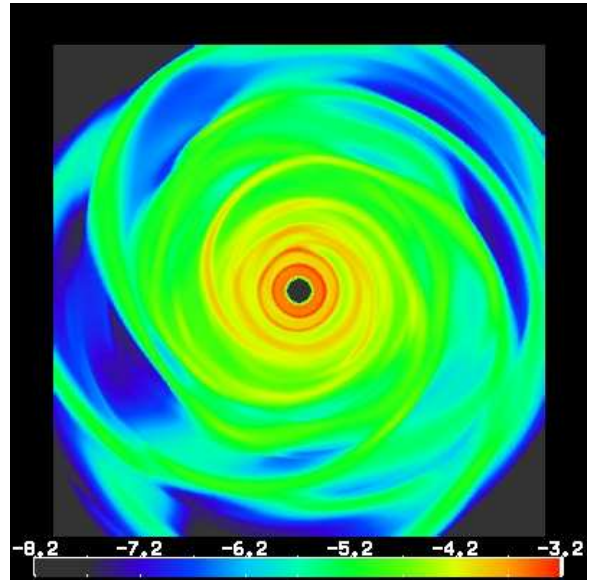


Figure 3: Equatorial density plot for moderate simulation. Scale is logarithmic in arbitrary units. Multiplying by 7.4×10^{-7} gives g/cc. Snapshot is taken at the end of the simulation, in this case about 4750 years. The panel is approximately 100 AU on a side.

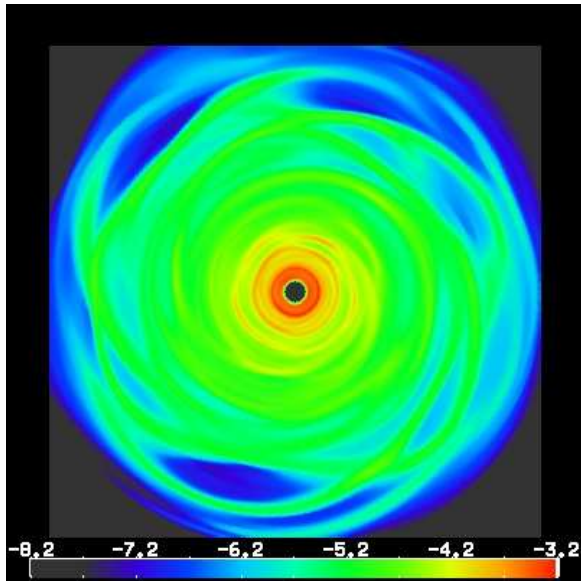


Figure 2: Equatorial density plot for steep simulation. Scale is logarithmic in arbitrary units. Multiplying by 6.67×10^{-7} gives g/cc. Snapshot is taken at the end of the simulation, in this case about 4500 years. The panel is approximately 100 AU on a side.

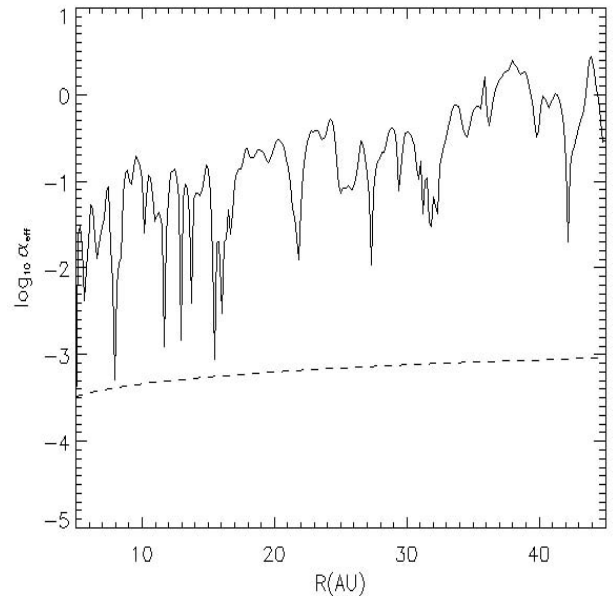


Figure 4: Comparison of calculated α (solid) to Gammie's α (dashed) for the steep simulation.